Electronic Supplementary Information

Supramolecular Combinations of Fractionated Humic Polyanions as Potent and Cost-Effective Microbicides with Polymodal anti-HIV-Activities and Low Cytotoxicity

Yury V. Zhernov, [1], Stephan Kremb,[2] Markus Helfer,[2] Michael Schindler,[3] Mourad Harir,[4] Constanze Mueller,[4] Norbert Hertkorn,[4] Nadezhda P. Avvakumova,[5] Andrey I. Konstantinov,[6] Ruth Brack-Werner,[2] Philippe Schmitt-Kopplin,[4,7] and Irina V. Perminova[6*]

1. Institute of Immunology of the Federal Medical-Biological Agency of Russia, Moscow, Russia

2. Institute of Virology, Helmholtz Zentrum München - German Research Center for Environmental Health, Neuherberg, Germany

3. University Hospital Tübingen, Institute for Medical Virology and Epidemiology of Viral Diseases, Tübingen, Germany

4. Research Unit Analytical BioGeoChemistry, Helmholtz Zentrum München - German Research Center for Environmental Health, Neuherberg, Germany

5. Department of General, Bioinorganic and Bioorganic Chemistry, Samara State Medical University, Samara, Russia

6. Department of Chemistry, Lomonosov Moscow State University, Moscow, Russia

7. Technical University of Munich, Division of Analytical Food Chemistry, Freising-Weihenstephan, Germany

*Phone/Fax: +7(495)9395546 ; E-mail: iperm@org.chem.msu.ru

Tables - 3

Figures – 8

Isolation and fractionation of the humic PAs from native peloids.

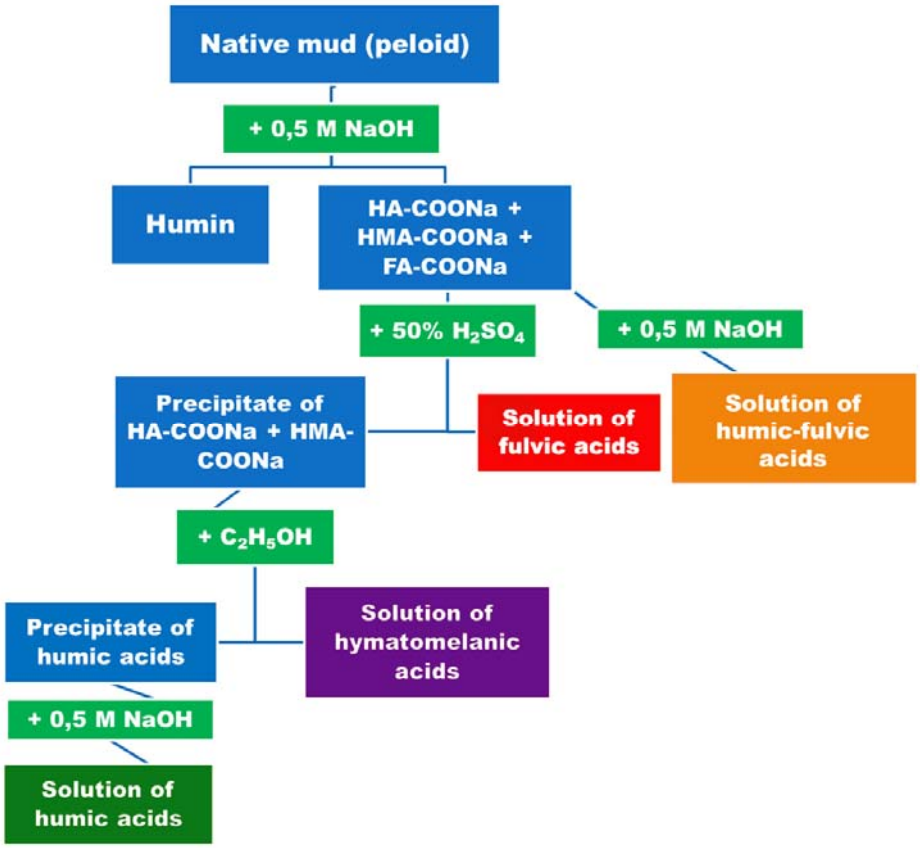

Figure S1. Fractionation scheme of the initial humic substances extract (HFA) into fractions of humic acids (HA), fulvic acids (FA) and hymatomelanic acid (HMA).

To estimate hydrophobicity of the humic PAs under study, we used RPLC measurements. The typical RPLC profiles are given in Fig. S2.

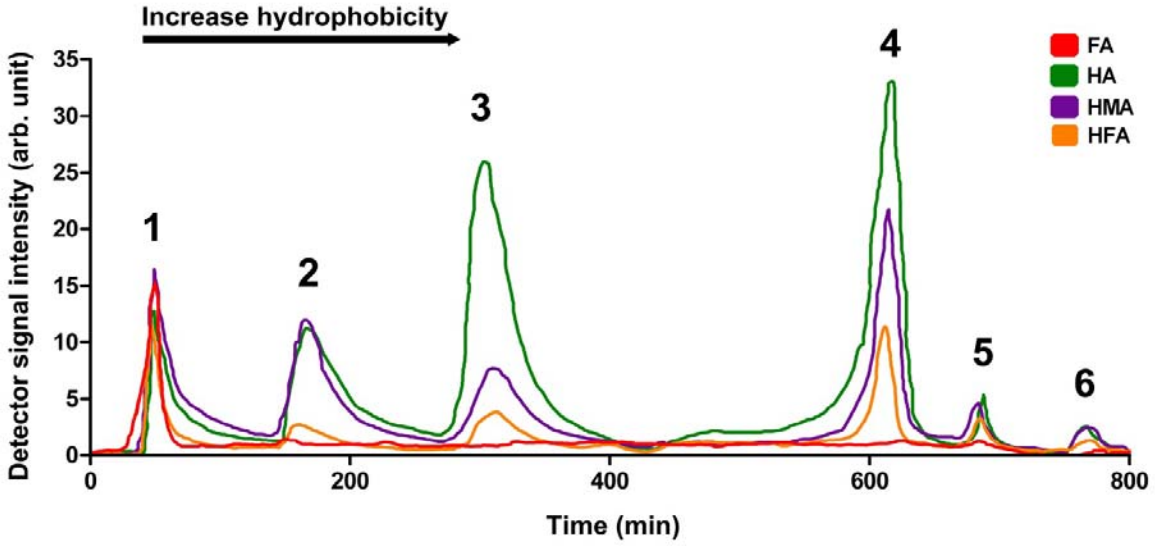

Figure S2. The PRLC profiles of the humic PAs used in this study. The chromatographic column dimensions 6×1 cm, column packing Octyl Sepharose CL-4B. The elution rate is 50 ml/h. Detection wavelength is 280 nm.

As it follows from Fig. S2, the humic PAs under study is represented by six peaks in the RPLC profiles: the first three are referred as hydrophilic, and the last three as hydrophobic ones. The evaluation of the corresponding chromatograms for the humic PAs under study are given in Table S1.

Table S1. Peak areas in the RPLC profiles of the humic PAs under study.

	1	2	3	4	5	6
	Peak values					
FA	82.42%	6.04%	-	6.05%	5.49%	-
HA	9.3%	17.04%	35.78%	33.59%	2.43%	1.85%
HMA	23.35%	23.35%	17.94%	28.3%	4.14%	2.93%
HFA	23.66%	13.35%	20.7%	32.14%	7.19%	2.96%

FA fraction is characterized by the presence of only one peak in the region of the highest hydrophilicity (the peak number 1 in Fig. S2) with an area of 88.46%. This is consistent with high solubility of this fraction in the whole range of pH values. HA has the highest percentage of

hydrophobic molecules and is characterized with 4 peaks: the largest one (number 4) is located in the hydrophobic region and comprise 73.7% of the total area. The composition of HFA is characterized by the presence of both hydrophilic and hydrophobic moieties with prevailing contribution of hydrophobic fractions, which comprise 63 % of the total area. HMA is the most amphiphilic fraction characterized by the presence of six peaks whose areas are almost equally distributed between hydrophilic and hydrophobic fraction. The total area of hydrophobic fractions is 53.3%. The molecular composition of HMA is narrower as compared to HA while it is a subfraction of HA. This is consistent with the reported data by Grimalt et al (1989). However, a substantial part of hydrophobic molecules remains in the HA fraction after ethanol extraction.[1] The given data were used for calculation of hydrophobicity index (HI) which represents contribution of hydrophobic peaks (number 4 to 6) into the total area of the RPLC chromatogram. Based on the HI value, the humic PAs under study might be arranged in the following order: HA > HFA > HMA > FA.

[1]Grimalt, J.O., Hermosín, B., Yruela Guerrero, I., Sáiz-Jiménez, C. Lipids of soil humic acids. II. Residual components after hymatomelanic acid extraction. Sci. Total Environ. 81-82: 421-428 (1989). doi: 10.1016/0048-9697(89)90150-2

To estimate structural group composition of the humic PAs under study they were analyzed using quantitative 13C NMR spectroscopy (solution state). The spectra obtained are shown in Fig. S3.

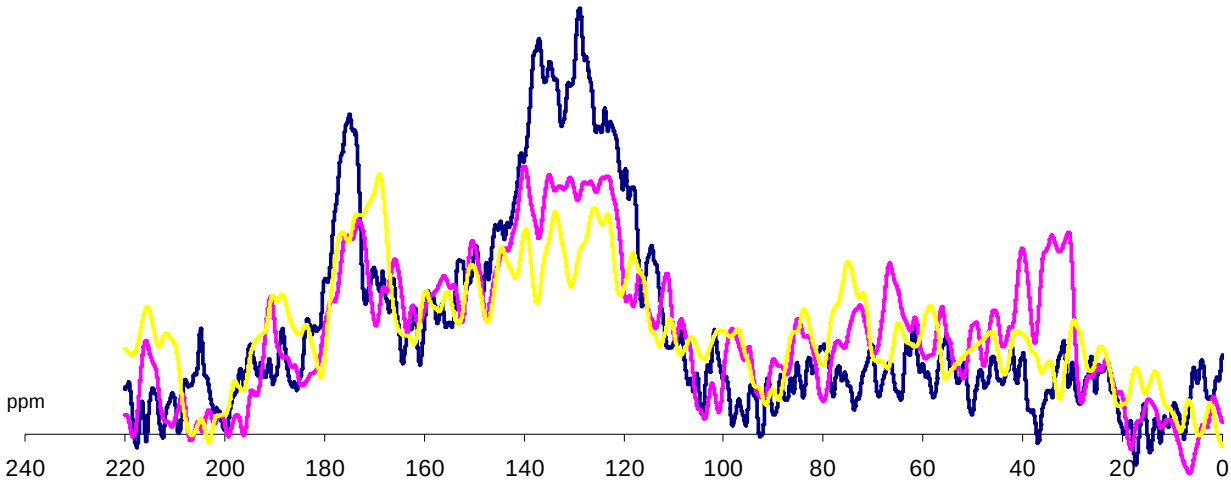

Figure S3. ^{13}C NMR spectra of three humic PAs under study highlighted in following colors: yellow – FA, purple – HMA, dark blue – HA.

Quantitative ^{13}C solution-state NMR spectra were recorded on an Avance NMR spectrometer (Bruker, Germany) operating at 100 MHz carbon-13 frequency. A 50 mg HA sample was dissolved in 0.6 mL 0.3 N NaOD and transferred into a 5 mm NMR tube. ^{13}C NMR spectra were acquired with a 5-mm broadband probe, using CPMG pulse sequence with nuclear Overhauser effect suppression by the INVGATE procedure; the acquisition time and relaxation delay were 0.2 s and 7.8 s, respectively. These conditions allowed quantitative determination of carbon distribution among the main structural fragments of HA. The assignments were as follows (in ppm): 5–48 carbon of non-substituted aliphatic fragments (CH_n), 48-54 – carbon of methoxyl groups (CH3O), 54 – 64 – carbon of O-substituted methylene groups (CH2O), 68-98 – carbon of CHO-groups (CHO), 98-108 – carbon of acetal groups (OCO), 108–165 - aromatic non-substituted carbon (Car), 165–187 – aromatic carbon substituted with O--containing functional groups (CarO), 165 – 187 - carboxylic and ester groups (C_{COO}); 187 – 220 - C atoms of quinonic and keto- groups ($C_{C=O}$).

Table S2. Distribution of carbon between main structural fragments of the humic PAs as measured by 13C NMR spectroscopy (in % of the total spectral density)

Humic PAs	CHn	CH3O	CH2O	CHO	OCO	Car	CarO	COO	C=O
HA	9.5	2.3	2.0	6.8	4.3	41.5	12.3	15.3	6.0
HMA	15.2	4.0	2.1	12.1	5.4	33.9	9.3	12.7	5.2
FA	12.1	2.7	3.2	12.8	8.1	25.8	9.6	15.1	10.7

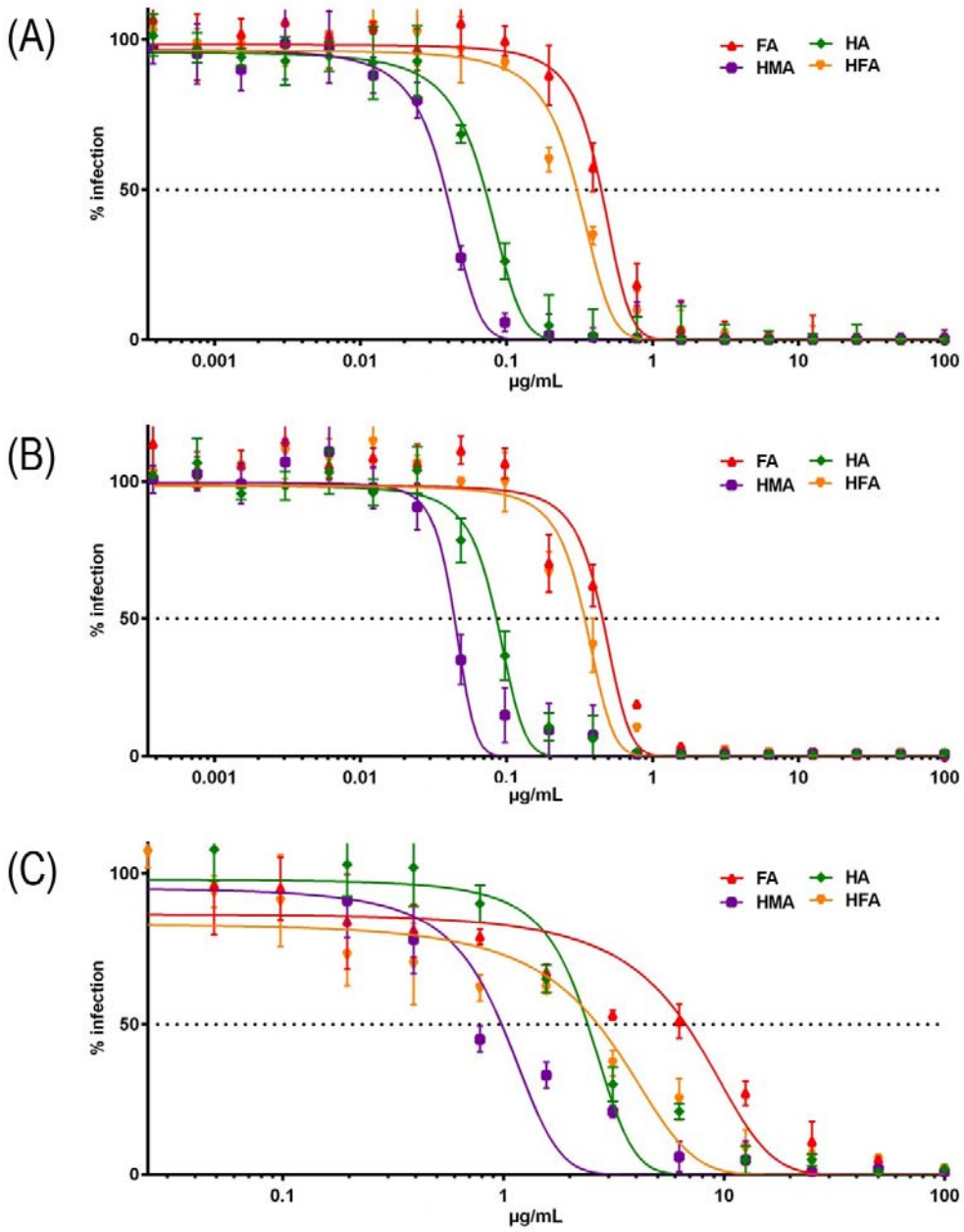

Figure S4. Dose-response curves for inhibition of HIV-1 infection of LC5-RIC cells by the humic PAs: (A) step 1 of EASY-HIT; (B) step 2 of EASY-HIT, and (C) PBMC. For EASY-HIT: n=9; R^2>0.9. For PBMC-based infection assay: n=3; R^2 > 0.9. The samples are shown as follows: FA (red triangles), HA (green circles), HMA (violet quadrants), HFA (orange triangles).

MTT test. Cell viability was assessed using MTT test. The protocol was used as proposed by Kremb et al.[55] The MTT assay measures ability of cells to reduce tetrazolium dye 3-(4,5-dimethylthiazol-2-yl)-2,5-diphenyltetrazoliumbromide (MTT) to its insoluble formazan form, which has a purple color. This conversion requires that mitochondria would be functioning, that is, present in the living cells. As a result, the MTT test effectively measures the metabolic activity of live cells. In our experiments, the cells were analyzed using MTT test 48 h after infection with HIV-1. The cell cultures were incubated with 100 µL of MTT solution (0.5 mg of MTT; Sigma, Taufkirchen, Germany) in 100 µL of culture medium for 2 h under standard culture conditions. MTT solution was carefully removed, and cells were lysed by addition of 100 µL of lysis solution (10% SDS and 0.6% acetic acid in dimethyl sulfoxide). The released formazan crystals were dissolved by gentle agitation, and formazan concentration was determined using a Tecan Infinite M200 analyzer at a wavelength of 570 nm and a reference wavelength of 630 nm. The cells treated with PAs, MTT, and lysis solution were used as positive controls for cytotoxicity. The intact cells, which were not treated with MTT and lysis solution, were used as negative controls. The cultural medium without cells and lysis solution was used as a blank. The toxicity values obtained for the HS-treated HIV-infected cultures were related to those of untreated, HIV-infected cultures in the same plate.

The results of MTT tests for the humic PAs under study are shown in Fig. S4.

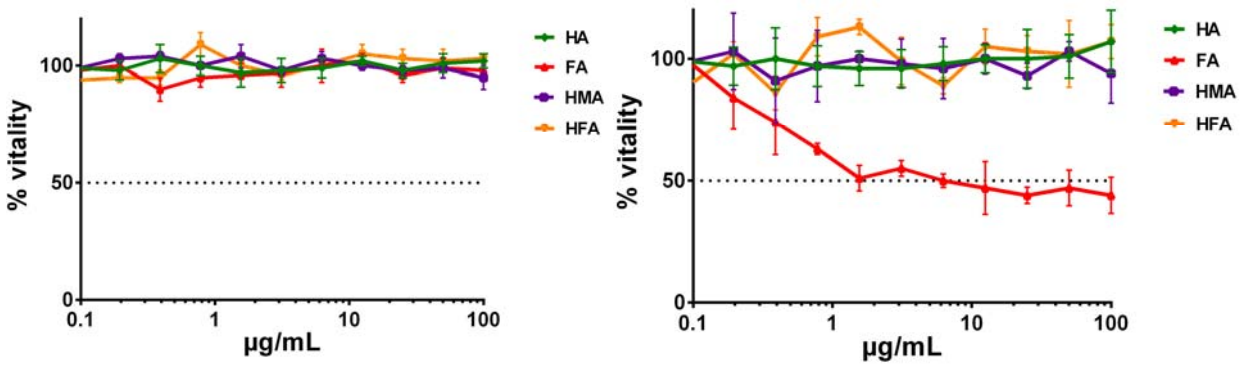

A **B**

Figure S5. Dose-response curves for LC5-RIC cells toxicity (A) and PBMC toxicity (B) by HS fractions: n=3; R^2>0.9.

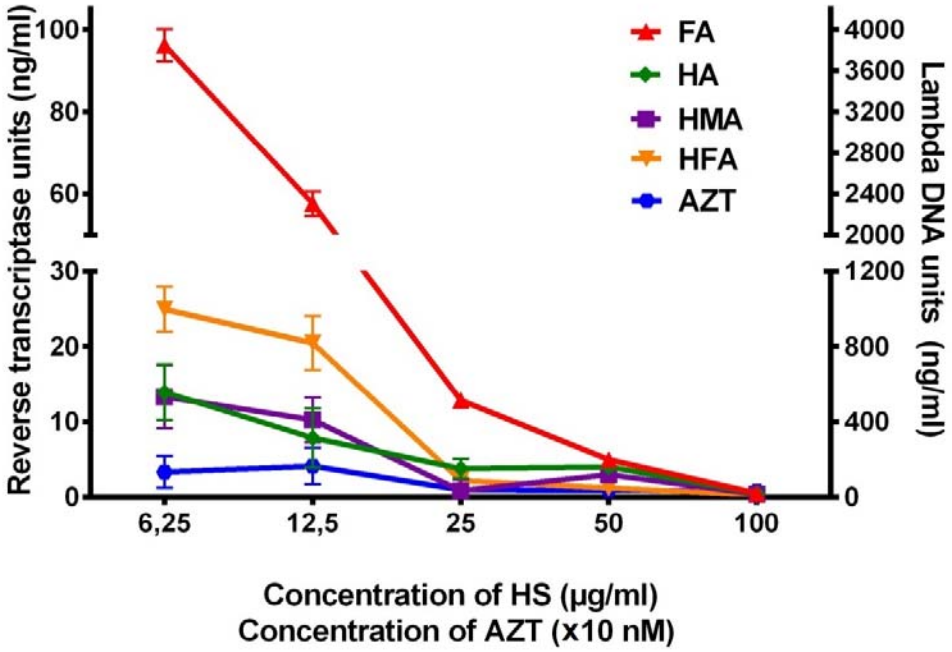

Figure S6 – Copy of Figure 3B in high resolution format.

Inhibition of virus attachment to host cells by the humic PAs in the presence of fusion inhibitor T-20 (fluorescence tagged virus particles, R5 HIV-1 NL4-3 Gag-iGFP, green, and LC5-RIC-R5 cells) as determined by fluorescent imaging (A) and reverse transcriptase inhibition activity of the humic PAs (B), which are color-coded as follows: FA (red), HA (green), HMA (violet), HFA (orange) (n=3; R^2 > 0.9). AZT (the reference) is shown in blue.

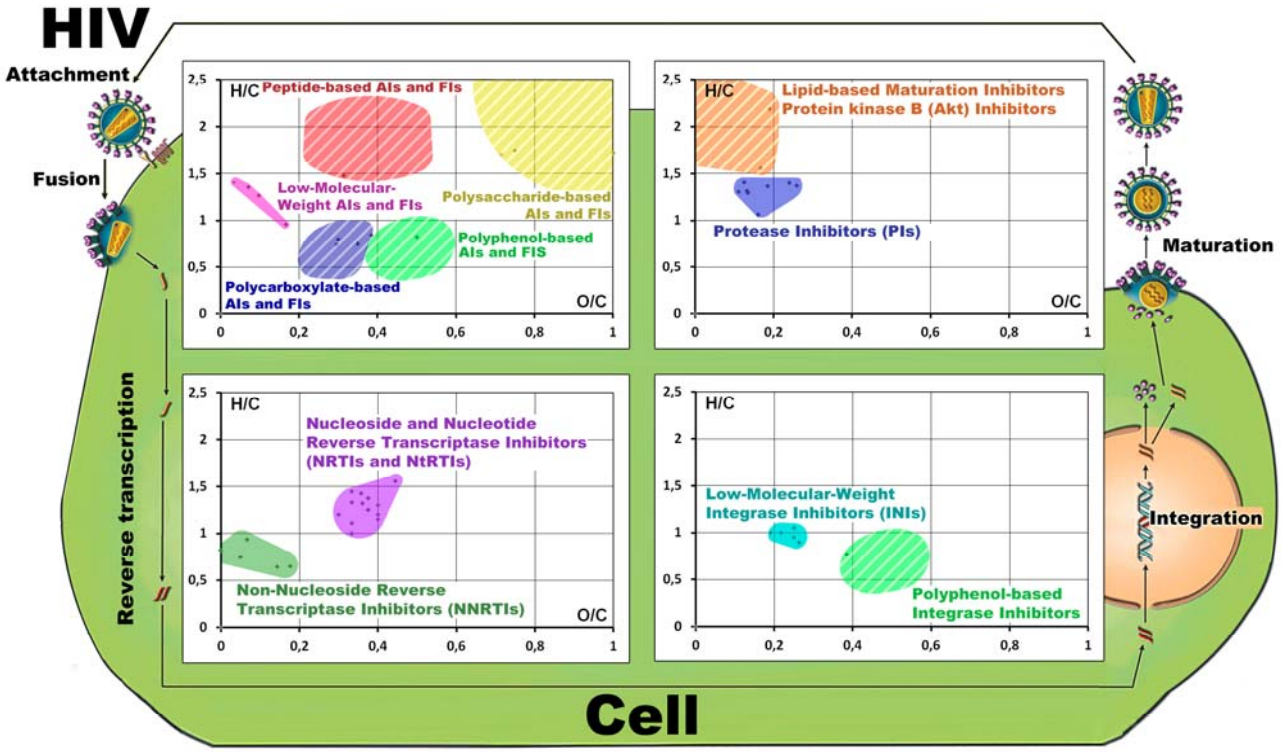

Figure S7. Molecular space of four different classes of antiretroviral compounds plotted in the Van Krevelen diagrams positioned respectively along the HIV-life cycle. The upper diagram in the left panel of the figure shows subspace of attachment and fusion inhibitors (AIs and FIs) including low molecular weight AIs and FIs (purple filed), peptide based AIs and FIs (shaded red field), polycarboxylate PAs (shaded blue field), sulfonated/sulphated polysascharide PAs (shaded yellow filed), polyphenol-based PAs (shaded light green field). The bottom VK diagram in the left panel shows subspaces of Nucleoside and Nucleotide Reverse transcriptase inhibitors (NRTIs and NtRTs) (violet color) and Non-Nucleoside Reverse transcriptase inhibitors (NNRTIs) (dark green). The bottom VK diagram on the right shows subspaces of integration inhibitors: monomolecular approved drugs (turquoise) and polyphenol based compounds (green); and the subspaces of maturation and protease inhibitors (MIs and PIs, respectively) and shown in the upper VK diagram in the right using orange and dark blue color, respectively.

Table S3. Atomic compositions and masses of antiretroviral drugs used for mapping Van Krevelen diagrams shown in Fig. S6.

Classes of drugs	Drug name	Mass	H	C	O	N	S	O/C	H/C
Nucleoside Reverse Transcriptase Inhibitors (NRTIs)	**Abacavir sulfate**	286,332	20	14	5	7	0	0,36	1,43
	Emtricitabine	247,248	10	8	3	3	1	0,38	1,25
	Lamivudine	229,26	11	8	3	3	1	0,38	1,38
	Didanosine	236,227	12	10	3	4	0	0,3	1,2
	Zidovudine	267,242	13	10	4	5	0	0,4	1,3
	Apricitabine	229,256	11	8	3	3	1	0,38	1,38
	Stampidine	544,289	23	20	8	3	0	0,4	1,15
	Elvucitabine	227,19	10	9	3	3	0	0,33	1,11
	Racivir	247,25	10	8	3	3	1	0,38	1,25
	Amdoxovir	252,23	12	9	3	6	0	0,33	1,33
	Stavudine	224,213	12	10	4	2	0	0,4	1,2
	Zalcitabine	211,218	13	9	3	3	0	0,33	1,44
	Festinavir	248,235	12	12	4	2	0	0,33	1
Nucleotide Reverse Transcriptase Inhibitors (NtRTIs)	**Tenofovir disoproxil fumarate**	287,213	14	9	4	5	0	0,44	1,56
	Tenofovir alafenamide fumarate	592,53	33	25	9	6	0	0,36	1,32
Non-Nucleoside Reverse Transcriptase Inhibitors (NNRTIs)	**Efavirenz**	315,675	9	14	2	1	0	0,14	0,64
	Nevirapine	266,888	14	15	1	4	0	0,07	0,93
	Delavirdine	456,562	27	22	3	6	1	0,14	1,23
	Etravirine	435,28	15	20	1	6	0	0,05	0,75
	Rilpivirine	366,42	18	22	0	6	0	0	0,82
	Doravirine	425,75	11	17	3	5	0	0,18	0,65
Entry/fusion inhibitors	**Enfuvirtide**	4492,1	301	204	64	51	0	0,31	1,48
	Maraviroc	513,666	41	29	1	5	0	0,034	1,41
	Vicriviroc	533,629	38	28	2	5	0	0,07	1,36
	Cenicriviroc	696,95	52	41	4	4	1	0,098	1,27
	Temsavir	583,5	23	24	4	7	0	0,17	0,96
Integrase strand transfer inhibitors (INSTI)	**Raltegravir**	444,42	21	20	5	6	0	0,25	1,05
	Elvitegravir	447,883	23	23	5	1	0	0,22	1
	Dolutegravir	419,38	19	20	5	3	0	0,25	0,95
	Globoidnan A	492,44	20	26	10	0	0	0,38	0,77
	MK-2048	461,87	21	21	4	5	0	0,19	1
	BI 224436	391,46	25	24	4	1	0	0,17	1,04
	Cabotegravir	405,36	17	19	5	3	0	0,26	0,89
Maturation inhibitors	Bevirimat	584,826	56	36	6	0	0	0,17	1,56

Protease Inhibitors (PIs)	**Fosamprenavir**	585,608	36	25	9	3	1	0,36	1,44
	Lopinavir	628,81	48	37	5	4	0	0,14	1,30
	Nelfinavir	567,784	45	32	4	3	1	0,12	1,41
	Ritonavir	720,946	48	37	5	6	2	0,13	1,30
	Saquinavir	670,841	50	38	5	6	0	0,13	1,32
	Amprenavir	505,628	35	25	6	3	1	0,24	1,40
	Indinavir	613,79	47	36	4	5	0	0,11	1,31
	Atazanavir	704,856	52	38	7	6	0	0,18	1,37
	Darunavir	547,665	37	27	7	3	1	0,26	1,37
	Tipranavir	602,66	33	31	5	2	1	0,16	1,06
Pharmacokinetic Enhancers (Boosters)	Ritonavir	720,946	48	37	5	6	2	0,13	1,30
	Cobicistat	776,023	53	40	5	7	2	0,13	1,33
Polycarboxylate-based AIs and FIs	CSty-alt-MAn	247,2249	11	13	5	0	0	0,38	0,85
	CSty-alt-CPMI	366,3474	16	20	6	1	0	0,30	0,80
	DCSty-alt-MAn	367,3315	15	20	7	0	0	0,35	0,75
	DCSty-alt-CPMI	486,454	20	27	8	1	0	0,30	0,74

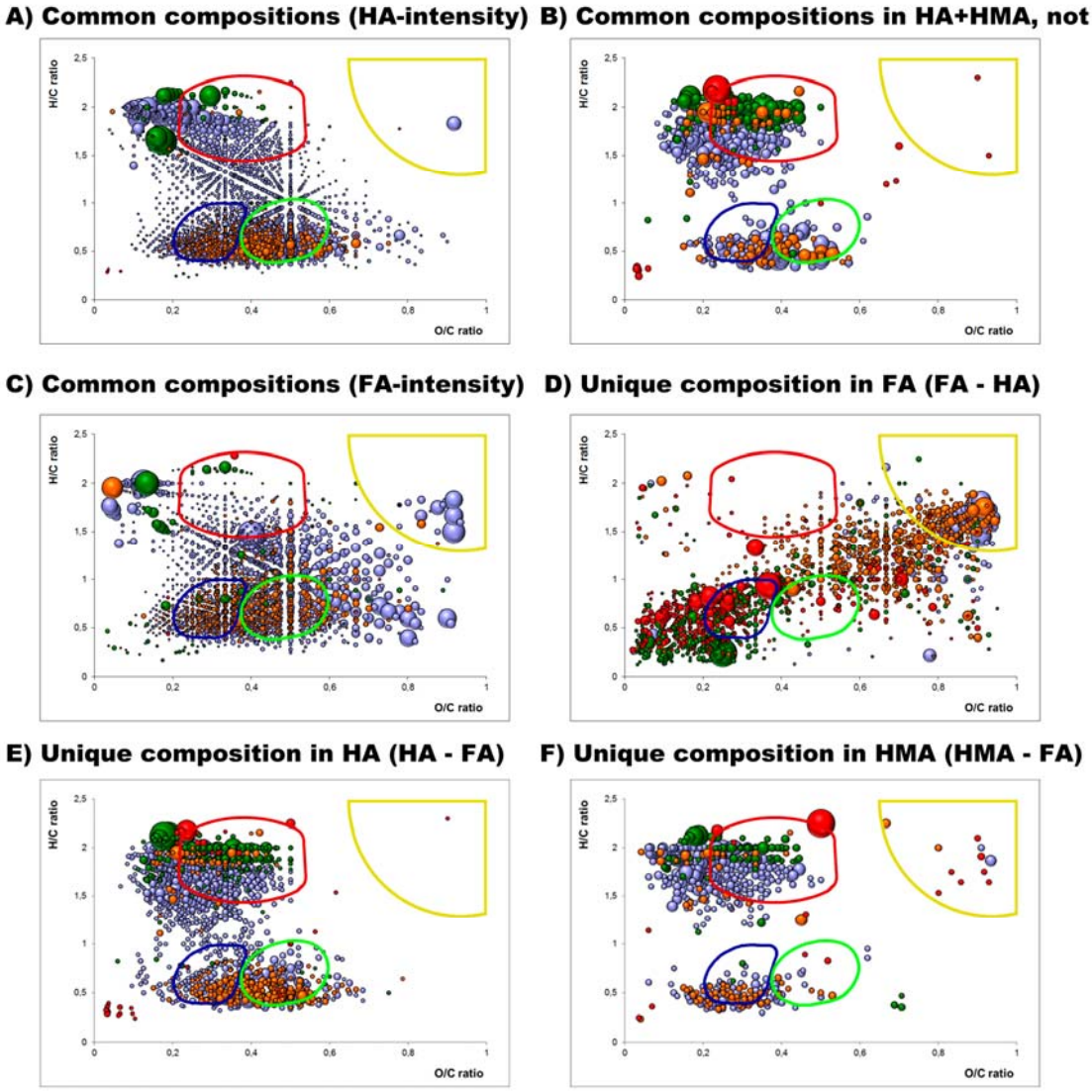

Figure S8. Common and unique molecular pools of the humic PAs under study and their overlap with the molecular space of other chemical classes of PAs. A) Molecules present in all three fractions with the intensity of HA; B) Common molecules present in HA and HMA; C) Common molecules for all three fractions with intensity of FA; D) Unique molecules present only in FA; E) Unique molecules present only in HA; F) Unique molecules present only in HMA. The shaded areas: red color - high molecular weight peptides; blue color – synthetic polycarboxylates, green color – polyphenols PAs, yellow color – polysaccharides.